CHAPTER IV

Development of Poly(p-phenylene)/ Crosslinked Poly(ε-caprolactone) as Electroactive Shape Memory Composite

Napat Charoonrak[a]. Anuvat Sirivat[a*], Wanchai Lerdwijitjarud[b]

[a]*The Petroleum and Petrochemical College, Chulalongkorn University, Bangkok, 10330, Thailand.*

[b]*Department of Materials Science and Engineering, Faculty of Engineering and Industrial technology, Silpakorn University, Nakorn Pathom 73000, Thailand.*

anuvat.s@chula.ac.th

4.1 Abstract

Electroactive shape memory composites consisting of iron (III) chloride ($FeCl_3$) doped poly(p-phenylene) (PPP)/crosslinked poly(ε-caprolactone) (cPCL) were fabricated using benzoyl peroxide (BPO) as a crosslinking agent. Then, the electromechanical properties of the poly(ε-caprolactone) (PCL) film and the composite under the effects of crosslinking ratio and concentration of embedded PPP were investigated. For the electromechanical properties, 3% wt BPO cPCL exhibits the highest storage modulus response and storage modulus sensitivity. In case of the PPP/PCL system, the storage modulus response and storage modulus sensitivity decrease dramatically at the PPP concentration of 0.01% v/v, then increase with increasing PPP concentrations from 0.05, 0.1, 0.5 to 1% v/v. For the deflection experiment, both of the pure cPCL and PPP/PCL system bend towards the positive electrode. Moreover, the deflection angle and dielectrophoresis force on the samples increase linearly with increasing the electric field.

Keywords: Electroactive polymer, Shape memory composite, Conductive polymer, Crosslinked polycaprolactone, Poly(p-phenylene)

*Corresponding author Tel.: +662 218 4131; Fax: +662 611 7221

4.2 Introduction

Electroactive materials are smart materials that can provide large amounts of deformation in the presence of applied electric field [1]. There are myriad of applications from shape memory materials [2] to robotic application [3]. Electroactive polymers (EAPs) are attracting the attention of scientists and engineers for development and fabrication for decades because of their lightweight, relatively low cost, good corrosion resistance, more flexibility, fast response and large strain under electrical stimulation [4,5].

Polycaprolactone (PCL), rubber-like, hydrophobic and semi-crystalline synthetic polyester was discovered by Carothers group in 1930s. In the present, PCL is the potent material for biomedical applications such as suture, wound dressing, medical splint, because of its low melting temperature (58-64 °C), biodegradability, high rigidity and high modulus of elasticity [6,7]. Normally, the mechanical strength drops dramatically above the melting temperature, so crosslinking is required to enhance both thermal and mechanical properties [8]. Radical crosslinking is the useful method because of low cost, available easily and take a short time period [9,10].

For an electroactive application, electroactive fillers such as carbon nanotubes (CNTs), carbon particles, and electromagnetic fillers are required to drive this unique effect [11]. For instance, a carbonous filler was embedded into polyurethane and coated with polypyrrole for fabricating a shape memory composite [12]. The electrical conductivity of the composite increases up to 8 orders of magnitude and the electroactive recovery effect occurs when a constant voltage of 25 V was applied.. Poly(p-phenylene) (PPP), the well-known conductive polymer which was blended in an acrylic elastomer to investigate the electroactive properties [13]. Both electrical conductivity and electromechanical properties such as storage modulus response and electrical sensitivity increase linearly with increasing PPP concentration.

Typically, the electrical conductivity of undoped conductive polymers are quite low, so a doping process with a variety of dopants such as alkali metals, arsenic pentafluoride (AsF_5), antimony pentachloride ($SbCl_5$) and iron (III) chloride ($FeCl_3$)

is required for enhancing the conductivity [14,15]. Doping with $FeCl_3$ is one of the most popular way because it is the least harmful dopant and relatively of greater stability when compared with other dopants [16].

In present work, poly(p-phenylene) (PPP) was synthesized via the the oxidative polymerization with poly(ε-caprolactone) (PCL). Influences of degree of crosslinking via a radical crosslinking, doping level by varying concentration of the dopant, iron (III) chloride ($FeCl_3$), and concentration of embedded PPP on thermal, electrical conductivity and electromechanical properties under and not under electric field were investigated and reported here.

4.3 Experimental

4.3.1 Materials

Benzene (LOBA Chemie, ACS agent, 99.5% purity) was used as a monomer for synthesizing PPP and a solvent for PCL film casting. Anhydrous aluminium chloride ($AlCl_3$) (Sigma Aldrich, AR grade, 98% purity) and anhydrous cupric chloride ($CuCl_2$) (Aldrich, AR grade, 97% purity) were used as an oxidizing agent and a catalyst, respectively. Anhydrous iron (III) chloride ($FeCl_3$) (Sigma Aldrich, AR grade, 97% purity) and absolute ethanol (RCI Labscan, AR grade, 99.9% purity) were used as a dopant and a solvent for dopant, respectively. Hydrochloric acid (RCI Labscan, AR grade, 37%) was used as a filtrant. Benzoyl peroxide (BPO) (Aldrich, Luperox® A75, 25% reminder water) was used as a PCL crosslinking agent. Polycaprolactone (PCL) (M_n = 70,000-90,000 by GPC, Aldrich, AR grade) was used as the polymer matrix. All chemicals were use without further purification.

4.3.2 Synthesizing of Poly(p-phenylene) (PPP)

Poly (p-phenylene) was synthesized via the cationic polymerization method by using benzene, anhydrous aluminium chloride ($AlCl_3$), and anhydrous cupric chloride ($CuCl_2$) with the mole ratio of 1:0.5:0.5 respectively [13]. The reaction occurred in a 3-neck round-bottom flask at 37 °C for 4 hours. Then the solution was filtered with hot 18% hydrochloric acid and finally in hot DI water at 80 °C until it had a pH of 6.0. At last, undoped PPP (uPPP) powder was dried at 100 °C for 24 hours. A light brown solid powder was finally obtained [17].

4.3.3 PPP Doping Process

The PPP particles were immersed in $FeCl_3$-absolute ethanol mixture at 60 °C in a 1:50, 1:30, 1:1, 30:1, 50:1 and 100:1 mole ratios between $FeCl_3$ and PPP monomer. The mixtures were stirred for 48 hours before filtration using the Buchner funnel connected with a vacuum pump. The doped PPP (dPPP) was dried at 100 °C for 24 hours [18,19,20].

4.3.4 Poly (ε-caprolactone) (PCL) Film casting and PCL Crosslinking

PCL was dissolved in benzene and mechanically stirred for 2 hours before casted on a glass plate for 24 hours at room temperature. Finally, dried PCL film was obtained. In case of crosslinked PCL film, PCL was dissolved in benzene before 1, 3, 5, 7 and 10 wt% of BPO were added in the solutions under stirring for 2 hours at room temperature [10]. Then the solutions were casted on glass plates and dried at room temperature for 24 hours. The completely dried PCL was cured in an oven at 130 °C for 5 min to obtain crosslinked PCL films [8].

4.3.5 PCL and PPP composite fabrication

uPPP and dPPP, were added in 0.01, 0.05, 0.1, 0.5, and 1 % v/v into the PCL and cPCL solutions. The particles were mechanically dispersed by vigorous stirring for 3 hours. Then they were dried at room temperature for 24 hours. Finally, the completely dried PCL was kept in an oven at 130 °C for 5 min as the curing temperature to obtain crosslinked PCL films embedded with PPP particles.

4.3.6 Characterization methods

Chemical structure of PPP particle was investigated by a Fourier transform infrared spectrometer (FT-IR) (Thermo Nicolet, Nexus 670). The spectrometer was operated in the transmission mode averaging 64 scans at a resolution of 4 cm^{-1}, covering a wave number range of 4,000–400 cm^{-1} [21]. Optical grade potassium bromide (KBr) was used as a background material. Firstly, KBr was heated at 100 °C for 24 hours for dehydration before mixed with the particle in the ratio of 1:20.

The morphology of PCL and cPCL films and distribution of the particles in the composites were investigated by a scanning electron microscope (SEM) (Hitachi,

S8400). A small cross-section cut sample was placed on a sample holder and sputter coated with platinum [22].

Electrical conductivity of uPPP, dPPP, PCL film, and PPP/PCL composites were measured by a two-point probe connected with a voltage supplier (Keithley, 6517A). The polymers were compressed into pellets at 10 tons with 1 cm diameter. A constant voltage was applied to the pellet and the current was simultaneously measured then calculated into electrical conductivity [23]. The electrical conductivity was calculated from this following equation

$$\sigma = (I/KVt) \qquad \text{(i)}$$

where σ is the electrical conductivity (S/cm), I is the measured current (A), V is the applied voltage (V), t is the thickness (cm), and K is the geometric correction factor of the two-point probe which was determined by calibrating the probe with a silicon wafer possessing a known resistivity value.

The electromechanical properties including storage modulus response ($\Delta G'$) and electrical sensitivity ($\Delta G'/G'_0$) with and without electric field were measured by a melt rheometer (Ares, Rheometric Scientific) which has a custom-built copper parallel plate fixture (diameter 25 mm). DC voltage was supplied by a DC power source (Tektronix, CDM250) that can provide up to 4 kV as the maximum voltage. Storage modulus was investigated as a function of electric field, which was varied from and 0.1 kV to 2 kV, and frequency, were varied from 0.1 to 100 rad/s.

The dielectrophoresis forces were determined the deflection distances in the vertical cantilever fixture under electric field. The specimens were vertically immersed in the silicone oil (viscosity=100 cSt) between parallel copper electrode plates (68 mm of length, 40 mm of width, and 2 mm of thickness). The gap between the pair of the electrodes will be 30 mm. A DC Voltage was applied with a DC power supply (Goldsun, GPS 3003B) connected to a high voltage power supply (Gamma High Voltage, model UC5-30P and UC5-30N) which can deliver and electric field up to 25 kV. A video camera was used to record the deflection during experiment. Photos were captured from the video and the deflection distances in x

(*d*) and y axes (*l*) at the end of the specimen were determined by using the SemAfore software (version 5.21). The electric field strength was varied between 0 and 500 V/mm at the room temperature. Both the voltage and the current were monitored. The resisting elastic force of the specimens was calculated under electric field using the non-linear deflection theory of a cantilever, which can be obtained from the standard curve between $(F_e l_0^2)/(EI)$ and d/l_0 (l_0 = initial length of specimens); F_e is the elastic force, d is the deflection distance in the horizontal axis, l is the deflection distance in the vertical axis, E is the Young's modulus which is equal to $2G'(1+\nu)$, where G' is the shear storage modulus taken to be $G'(\omega = 1$ rad/s) at various electric field strength and I is the moment of inertia $1/12t^3w$, where t is the thickness of the sample and w is the width of the sample. The electrophoresis force can be calculated from the static horizontal force balance consisting of the elastic force and the corrective gravity force term ($mg\sin\theta$), as shown in these following equations:

$$F_d = F_e + mg\sin\theta + \rho V g \sin\theta \text{ (N)} \qquad \text{(ii)}$$

where g is 9.8 m/s^2, m is the mass of the specimen, ρ is the density of the silicone oil and θ is the deflection angle [24].

4.4 Results & Discussion

4.4.1 Characterizations of uPPP, dPPP, PCL and PPP/PCL composite

The FT-IR spectrum of uPPP shows characteristic peaks at 689-805 cm^{-1}, 999 cm^{-1}, 1383-1479 cm^{-1}, and 3020-3030 cm^{-1} which can be attributed to the C-H out of plane vibration of the mono-substituted benzene ring, the C-C stretching of the benzene ring, the p-substitution of the benzene ring, and the C-H stretching of the benzene ring, respectively [25,20]. After the doping process, there are unique peaks in the range of 1057-1110 cm^{-1} and 1559-1572 cm^{-1} [18] which can be assigned to the intrinsic vibration of the polymer chains in the doped state.

The thermograms of uPPP and dPPP were measured by using the TGA technique. There is a dramatical weight loss around 660 °C, corresponding to the backbone decomposition of PPP. After the doping process, the rate of decomposition

is higher compared with the uPPP because of the defect of the dopant in the PPP backbone [18].

For the thermogram of PCL and cPCL matrix, the weight losses of the samples occur at approximately 384 and 368 °C. This can be attributed to the PCL chain decomposition. The decomposition temperature of cPCL is slightly smaller compared with the pure PCL because the crosslinking cause a reduction in the crystallinity [26]. At last, for the PCL/PPP composite, there is a dramatical weight loss at approximately 370 °C which is contributed to decomposition temperature of the composite. The final weight after the experiment increase linearly with the concentration of embedded PPP, corresponding to the incomplete degraded PPP particles.

Scanning electron microscope (SEM) was deployed to observe the microstructures of PPP particles and the morphology of PP/PCL composite. As shown in Fig. 4.1(a) and Fig. 4.1(b), the SEM image shows the irregular rod-like structure of PPP particles. Fig. 4.1 (c) and Fig. 4.1(d) show the morphology of the pure 3% wt BPO cPCL and 1.0% v/v 30:1 dPPP/cPCL respectively, showing that particles are dispersed uniformly in the cPCL matrix.

The electrical conductivities of uPPP and dPPP were measured by using custom-built two-point probe. The conductivity of synthesized uPPP is equal to 8.14×10^{-6} S/cm with a standard deviation of 8.73×10^{-7} S/cm. After the doping process with $FeCl_3$, The conductivity of 1:50 dPPP, 1:30 dPPP, 1:1 dPPP, 30:1 dPPP, 50:1 dPPP and 100:1 dPPP are 4.53×10^{-6}, 1.35×10^{-5}, 7.857×10^{-5}, 6.631×10^{-3}, 9.125×10^{-3} and 1.480×10^{-2} S/cm with standard deviations of 1.662×10^{-6}, 2.407×10^{-7}, 4.532×10^{-6}, 1.434×10^{-4}, 1.267×10^{-3} and 8.423×10^{-3} S/cm, respectively. The electrical conductivity increases with the concentration of the dopant. However, at a very high doping level, there are agglomerations of the dopant particles so the conductivity does not increase significantly.

4.4.2 Electromechanical properties of PCL and cPCL films

4.4.2.1 Influence of crosslinking ratio in the absence of electric field

Electromechanical properties of neat PCL and cPCL were first measured in the absence of electric field at the frequency of 100 rad/s. The initial storage modulus (G'_0) of the samples is inversely proportional to the crosslinking ratio [27,10]. The initial storage moduli of the neat PCL, 1% wt, 3% wt, 5% wt, 7% wt and 10% wt BPO cPCL are 631,730, 188,495, 108,688, 103,564, 95,223 and 87,781 Pa respectively. This can be explained that the crosslinking agent will restrict the crystalline packing in the casting process, corresponding to the reduction of the crystalline region in the sample and the initial storage modulus decreases respectively [8,26].

4.4.2.2 Influence of crosslinking ratio under electric field

Next, the electromechanical response of PCL films including the storage modulus response ($\Delta G'$) and the storage modulus sensitivity ($\Delta G'/G'_0$) of the samples at various crosslinking ratios in the presence of electric field strengths from 0 to 2 kV/mm were measured. In case of 10% wt BPO cPCL, the maximum electric field strength of 600 V/mm was applied as a lot of bubbles were generated due to the high amount of CO_2 decomposing from excess BPO degradation which caused the irregular film thickness and a short circuit occurred. The storage modulus generally increases as the electric field strength is increased. $\Delta G'$ of neat PCL, 1%wt BPO, 3%wt BPO, 5%wt BPO, 7%wt BPO and 10%wt BPO cPCL are 191,884, 170,235, 444,112, 190,765, 66,576 and 50,898 Pa respectively The storage modulus response of the neat PCL and lightly crosslinked (3% wt BPO) and heavily crosslinked (10% wt BPO) cPCL are shown in Fig. 4.2. The corresponding $\Delta G'/G'_0$ of neat PCL, 1%wt BPO, 3%wt BPO, 5%wt BPO, 7%wt BPO and 10%wt BPO cPCL are 0.30, 0.90, 4.08, 2.00, 0.64 and 0.28 respectively. $\Delta G'/G'_0$ of the neat PCL, lightly crosslinked (3% wt BPO) and heavily crosslinked (10% wt BPO) cPCL are shown in Fig. 4.3.

According to these values, it can be concluded that 3%wt BPO has the highest storage modulus response and storage modulus sensitivity, due to two synergized effects; the reduction of initial storage modulus compared with pure PCL and 1%wt BPO) because strain hardening is hindered, and 3%wt BPO is the suitable

crosslinking ratio where the chain scission effect does not occur due to excessive BPO. At higher crosslinking ratios (5%wt BPO, 7%wt BPO and 10%wt BPO cPCL), polarizable groups, the carbonyl group, and oxygen atoms can be damaged by radical attacking and they can decompose into carbon dioxide respectively, [26] so the electrostatic interaction is reduced.

4.4.3 Electromechanical properties of PPP/PCL composites

4.4.3.1 Influence of concentration of PPP particles in the absence of electric field

The effect of the PPP concentration in the PPP/PCL composite on the electromechanical properties was investigated subsequently in the absence of electric field. The 3%wt BPO cPCL and 30:1 dPPP were chosen to produce blends with PPP particles, corresponding to the highest storage modulus sensitivity compared with other crosslinking ratios and relatively high electrical conductivity respectively. In this work, 0.01, 0.05, 0.1, 0.5 and 1.0% v/v of dPPP were used to make the blends. The initial storage modulus of 0.01% v/v, 0.05% v/v, 0.1% v/v, 0.5% v/v and 1.0% v/v dPPP/cPCL are 129,848, 188,654, 185,395, 196,882 and 229,349 Pa respectively which can be concluded that PPP particles behave as a filler so the initial storage modulus becomes higher when increasing PPP concentration into the PCL matrix, similar to the previous work [30,31].

4.4.3.2 Influence of concentration of PPP particle under electric field

Electromechanical properties of the samples at the various PPP particle concentrations were measured under electric field strength from 0 to 2 kV/mm. The storage modulus response of 0.01 % v/v, 0.05 % v/v, 0.1 % v/v, 0.5 % v/v and 1.0 % v/v dPPP/cPCL at 2 kV/mm of electric field are 22,082, 38,911, 52,468, 66,130 and 195,719 Pa respectively and the corresponding storage modulus sensitivity are 0.17, 0.24, 0.28, 0.34 and 0.85 respectively. Fig. 4.4 and 4.5 show the storage modulus response versus frequency and the storage modulus sensitivity at the low, medium and high concentration of PPP in the cPCL matrix respectively. It can be observed that the electromechanical properties of the blendscomposite increase with the electric field strength and the concentration of embedded PPP.

The higher PPP composition in the cPCL matrix, the higher electromechanical response to the electric field is obtained, as shown in Table 4.1. At the very low volume fraction of PPP particles (0.01% v/v), the particles will act as filler [30,31]. In addition, the distance between particles is quite large so interparticular interaction cannot be effective [32]. Thus, the storage modulus response and storage modulus sensitivity of this particular blend system is lower compared with the pure cPCL system. At the higher PPP concentration, electrical polarization is a dominant effect due to the counterions ($FeCl_4^-$) on the doped PPP and the distances between particles become smaller in which the interparticular interaction can be effectively generated.

The comparison to previous work is shown in Table 4.2 [28,13,29]. 3% wt BPO cPCL is the most optimum condition. This neat PCL has the highest storage modulus sensitivity compared to other dielectric elastomers and composites under 2 kV/mm of electric field strength; this is attributed to the ester groups in the PCL chain which can generate the dipole moment and have a higher response to the electric field.

4.4.4 Time dependence of electromechanical response

The time sweep test of PCL and PPP/PCL blend were investigated under the electric field strength from 0 to 2 kV/mm which was turned on and off alternatively. As shown in Fig. 4.6, experiments were carried out in the linear viscoelastic regime at the %strain of 0.03 and frequency of 1 rad/s. In case of the cPCL film, the storage modulus increases rapidly and reaches the equilibrium state when the electric field is on. Then, the storage modulus decreases and reversibly turns to its original value without residue dipole moment when the electric field is off. Induction time or τ_{ind} is the period of time that required to increase the storage modulus to reach the equilibrium state when the electric field is turned on is equal to 57 s. Recovery time or τ_{rec} is the period of time that required for storage modulus to decay to its original value when the electric field is turned off equals to78 s.

The temporal response of 1.0% v/v PPP/cPCL blend also shows the reversible induction and reduction of the storage modulus without residue dipole moment when

the 2 kV/mm of electric field is turned on and off alternatively. The induction time and the recovery time are equal to 38 and 66 s, respectively.

4.4.5 Dielectrophoretic behavior

Finally, the dielectrophoretic behavior of PCL films and PPP/PCL blends were observed by the deflection experiment. The PCL film and the PPP/PCL blends were gripped and suspended vertically into the silicone oil bath. A DC electric field was applied through the parallel copper electrodes, as shown in Fig. 4.7(a). The experiment was recorded by using a video camera recorder. The length of the sample immersed in the silicone oil (l_0), the deflection displacement along x axis (a) and the deflection length (l'), deflection angle (θ) and dielectrophoresis force (F_d) were measured by an analysis program. Constant electrical fields of 0-500 V/mm were applied for each sample during the experiment.

When the electrical stimulus was applied, both of PCL films and PPP/PCL blends bended to the positive or anode electrode via an electronic polarization, as shown in Fig. 4.7(b), corresponding to the attractive forces between the positive electrode and the induced dipole moment of the carbonyl group (C=O), the lone-pair electrons from the oxygen atom in PCL chain, and the counterion ($FeCl_4^-$) from doped PPP particles which contribute to make the net dipole moment in the sample to become negative.

4.4.6 Influence of electric field strength to the deflection angle, induction time and recovery time

The induction time (τ_{ind}), the time for the sample required to deflect to its maximum displacement, and the recovery time (τ_{rec}) the time for the sample required to return to its original displacement under the electric field strength of 0, 100, 200, 300, 400 and 500 V/mm are shown in Table 4.5. In case of 3% wt BPO cPCL, the average τ_{ind} is 0.50, 1.85, 3.83, 4.64 and 6.10 s and the average τ_{rec} is1.50, 2.55, 4.38, 5.44 and 7.10 s. For 1.0% v/v PPP/cPCL, the average τ_{ind} is 0.86, 2.852, 3.89, 4.74 and 6.01 s and the average τ_{rec} is1.30, 3.18, 4.10, 5.24 and 6.35 s. The higher electric field strength applied, the higher induction time and recovery time are observed for both 3% wt BPO cPCL and 1.0% v/v PPP/cPCL. Fig. 4.8(a) and 4.8(b)

show the deflection of 3% wt BPO cPCL and 1.0% v/v PPP/cPCL with and without electric field respectively. The data suggest that the deflection angle becomes higher with increasing electric field. At 500 V/mm, the deflection angle of 3% wt BPO cPCL and 1.0% v/v PPP/cPCL reach the maximum value, 58.9° and 31.9° respectively.

The comparison of the dielectrophoretic behavior between the 3% wt BPO cPCL and 1.0% v/v PPP/cPCL to other electroactive materials from previous works [33] is shown in Table 4.4. The electrical yield strength; the minimum electric field strength required to generate the deflection of the material of the cPCL is 0.1 kV/mm which is relatively low; this is due to the high storage modulus sensitivity compare to others dielectric elastomers. Moreover, the deflection angle and the dielectrophoresis force of the cPCL are 58.7° and 0.459 mN respectively, which are relatively high compared with those values of SAR, SIS and SBR.

The deflection angle and the dielectrophoresis force of 1.0 v/v PPP/cPCL are 31.5° and 0.222 mN respectively which are higher than those of SIS and SBR but lower than those SAR due to the lower storage modulus sensitivity and higher initial storage modulus.

4.5 Conclusion

In this work, electromechanical properties of poly(ε-caprolactone) films and poly(p-phenylene)/poly(ε-caprolactone) were investigated by studying the effect of crosslinking ratio of PCL by using BPO as a crosslinking agent, and the effect of embedded PPP particle concentration on the dynamic modulus, storage modulus response and storage modulus sensitivity. For the effect of crosslinking ratio, the storage modulus sensitivity belongs to 3%wt BPO cPCL, which equal to 4.08. For the PPP/PCL system, the storage modulus sensitivity significantly decreases at the very low concentration of PPP (0.01% v/v) as PPP particles behaves as a filler. However, these values start to increase with increasing concentration of embedded PPP to 1.0% v/v. The material shows the reversible induction and recovery under the electric field; it is suitable candidate as an actuator. For the deflection experiment, Both of PCL and PPP/PCL systems bend toward the positive or anode side under

applied electric field. The deflection angle, the induction time, the recovery time, and dielectrophoresis force of the samples increase linearly the electric field strength varying from 0 to 500 V/mm.

4.6 Acknowledgement

The author would like to acknowledge the financial supports to AS from these following agencies: the Conductive and Electroactive Polymer Research Unit, Chulalongkorn University; Thailand Research Fund (TRF-RTA), and the Royal Thai Government (Budget of Fiscal Year 2555).

REFERENCES

[1] Snyder, A.J., Tews, A.M., Frecker M.I., Zhang, G. And Runt J.P. *Biomedical Applications of Electroactive Polymers*. The 5th International Conference on Intelligent Materials (2003).

[2] Koo, C.M. (2012). Electroactive Thermoplastic Dielectric Elastomers as a Ner Generation Polymer Actuators. Thermoplastic Elastomer, 400-416.

[3] Kim K.J. and Tadokoro, S. (2007). Electroactive Polymers for Robotic Application; artificial muscles and sensors, London: Springer-Verlag.

[4] Bar-cohen, Y. (2002), *Artificial Muscles using Electroactive Polymers (EAP); Current capabilities and challenges*, Proceedings of the SPIE Smart Structures and Materials Symposium, EAPAD Conference, San Diego, CA, USA.

[5] Vinogradov, A., Su, J., Jenkins, C. And Bar-cohen Y. (2006). *State-of-the-Art Developments in the Field of Electroactive Polymers*, MRS Proceedings, Vol. 889.

[6] Woodruff, M.A. and Hutmacher, D.W. (2010). The return of a forgotten polymer - Polycaprolactone in the 21st century. Progress in Polymer Science, 35, 1217-1256.

[7] Colwell, J.M. (2006). Synthesis of Polycaprolactone Polymers for Bone Tissue Repair. A thesis submitted for the degree of Doctor of Philosophy, School of Physical and Chemical Sciences, Queensland University of Technology.

[8] Han, C., Ran, X., Su, X., Zhang, K., Liu, N. And Dong L. (2007). Effect of peroxide crosslinking on thermal and mechanical properties of poly(ε-caprolactone), Polymer International, 56, 593-600.

[9] Pandini, S., Passera, S., Messori, M., Paderni, K., Toselli, M., Gianoncelli, A., Bontempi, E. and Riccò, T. (2012). Two-way reversible shape memory behaviour of crosslinked poly(ε-caprolactone). Polymer, 1-10.

[10] Xiao, Y., Zhou, S., Wang, L. and Gong, T. (2010). Electro-active Shape Memory Properties of Poly(ε-caprolactone)/Functionalized Multiwalled Carbon Nanotube Nanocomposite. Applied materials and interfaces, 2, 3506-3514

[11] Liu,Y., Lv, H., Lan, X., Leng, J. and Du, S. (2009). Review of electro-active shape-memory polymer composite. Composites Science and Technology, 69, 2064–2068.

[12] Sahoo, N.G., Jung Y.C., Yoo, H.J. and Cho, J.W. (2007). Influence of carbon nanotubes and polypyrrole on the thermal, mechanical and electroactive shape memory properties of polyurethane nanocomposites. Composite Science and Technology, 67, 1920-1929.

[13] Kunanuruksapong, R. and Sirivat, A. (2007). Poly(p-phenylene) and acrylic elastomer blends for electroactive application. Materials Science and Engineering A, 454–455, 453–460.

[14] Hérold, C. and Billaud, D. (1990). Electrochemical doping of polyparaphenylene with alkali metals in solid state cell. Solid State Ionics, 40/41, 985-987.

[15] Kumar, D. And Sharma, R.C. (1998). Advances in Conductive Polymers. Eur. Polym. J., 84, 1053-1060.

[16] Bonagamba, T.J., Bello, Jr. B., Giotto, M.V., Panepucci, H., Magon, C.J. and Campos, M.S. (1995). Iron doping effects on the high-resolution 13CNMR spectra of solid poly(para-phenylene). Synthetic Metals, 68, 103-108.

[17] Golovtsov, I. (2005). Modification of conductive properties and processability of polyparaphenylene, polypyrrole and polyaniline. Ph. D. Thesis on natural and exact sciences. Faculty of Chemical and Materials Technology Department of Materials Science, Tallinn university of technology.

[18] Phumman, P., Niamlang, S. and Sirivat, A. (2009). Fabrication of poly(p-phenylene)/zeolite composites and their responses towards ammonia. Sensors, 9, 8031-8046.

[19] Plocharski, J. and Wyciślik, H. (2000). Mixed conductivity in poly(p-phenylene) doped with iron chloride. Solid State Ionics, 127, 337–344.

[20] Sohn, J.I., Sung J.H., Choi, H.J. and Jhon, M.S. (2002). The Effect of Particle Concentration of Poly(p-phenylene) on Electrorheological Response. Journal of Applied Polymer Sciences, 84, 2397-2403.

[21] Li, S., Li, Z., Fang, X., Chen, G.Q., Huang, Y. and Xu, K. (2008). Synthesis and characterization of polyparaphenylene from cis-dihydrocatechol. Journal of Applied Polymer Science, 110, 2085–2093.

[22] Ludeelerd, P., Niamlang, S., Kunanuraksapong, R. And Sirivat, A. (2010). Effect of elastomer matrix type on electromechanical response of conductive

polypyrrole/elastomer blends. Journal of Physics and Chemistry of Solids, 71, 1243-1250

[23] Thongsak, K., Kunanuraksapong, R., Sirivat, A. And Lerdwijitjarud, W. (2011). Electroactive polydiphenylamine/poly (styrene-block-isoprene-styrene) (SIS) blends: Effect of particle concentration and electric field. Materials Science and Enginerring C, 31, 206-214.

[24] Kunchornsup, W. And Sirivat, A. (2012). Physically cross-linked cellulosic gel via 1-butyl-3-methylimidazolium chloride ionic liqiud and its electromechanical response. Sensors and Actuators A, 175, 155-164.

[25] Dubois, M., Naji, A. And Billaud, D. (2001). Electrochemical insertion of alkaline ions into polyparaphenylene: effect of the crystalline structure of the host material. Electrochimaca, 46, 4301-4307.

[26] Mo-Ling, C. (1999) *Polymers as low-temperature thermoplastic splinting material*, Master's Thesis, The Hong Kong Polytechnic University, Hong Kong.

[27] Yu, X., Zhou, S., Zheng, X., Guo, T., Xiao, Y. And Song, B. (2009). A biodegradable shape-memory nanocomposite with exellent magnetism sensitivity. Nanotechnology, 20, 1-9.

[28] Hiumtup, P., Sirivat, A. And Jamieson A.M. (2008). Electromechanical response of a soft and flexible actuator based on polyaniline particles embedded in a cross-linked poly(dimethyl siloxane) network. Materials Science and Engineering C, 28, 1044-1051

[29] Puvanatvattana, T., Chotpattananont, D., Hiumtup, P., Niamlang, S., Sirivat, A. And Jamieson A.M. (2006). Electric field induced stress moduli in polythiophene/polyisoprene elastomer blends. Reactive & Functional Polymers, 66, 1575-1588.

[30] Thipdech, D., Kunanuraksapong, R. And Sirivat, A. (2008). Electromechanical response of poly(3-thiopheneacetic acid)/acrylonitrile-butadiene rubbers. Polymer Letter, 2, 866-877.

[31] Tungkavet, T., Seetapan, N., Pattavarakorn, D. And Sirivat, A. (2011). Improvement of electromechanical properties of gelatin hydrogels by blending with nanowire polypyrrole: effect of electric field and temperature. Polymer International, 61, 825-833.

[32] Wichiansee, W. And Sirivat, A. (2009). Electrorheological properties of poly(dimethylsiloxane) and poly(3,4-ethylenedioxythiophehne)/poly(styrene sulfonic acid)/ethylene glycol blends. Materials Science and Engineering C, 29, 78-84.

[33] Kunanuruksapong, R. and Sirivat, A. (2011). Effect of dielectric constant and electric field strength on dielectrophoresis force of acrylic elastomers and styrene copolymers. Current Applied Physics, 11, 393-401.

Table 4.1 Electromechanical Properties of PPP/PCL composites

%v/v of PPP	Initial storage modulus (G'_0) (Pa)	Storage modulus response at 2 kV/mm ($\Delta G'_{2\ kV/mm}$) (Pa)	Storage modulus sensitivity ($\Delta G'/ G'_0$)
0	108,688	444,112	4.08
0.01	129,848	27,082	0.17
0.05	188,654	38,911	0.24
0.1	185,395	52,468	0.28
0.5	196,882	66,130	0.34
1.0	229,349	195,719	0.85

Table 4.2 The comparison of electromechanical properties between 3% wt BPO cPCL and other electroactive materials

Sample	Electric field strength (kV/mm)	ΔG′ (Pa)	ΔG′/ G'_0	Freq (rad/s)	T (K)	References
3% wt BPO cPCL	2	444,112	4.08	100	298	
SAR		56,742	1.48	1	300	Kunanurak sapong *et al.*, 2011
SBR		14,872	0.69		300	
SIS		5,062	0.10		300	
5% v/v PTh/PI-03		5,446	0.52	100	300	Puvanatvattana *et al.*, 2006
10% v/v PTh/PI-03		4,026	0.33		300	
30% v/v PTh/PI-03		33,857	0.44		300	
20% v/v PANi/ PDMS		26,243	0.10		300	Hiumtup *et al.*, 2008

Table 4.3 Influence of PPP concentration on the dielectrophoresis response in the PPP/PCL composite systems

%v/v of PPP	E (V/mm)	θ	F_d (μN)	τ_{ind} (s)	τ_{rec} (s)
0	0	0.00	0.00	0.00	0.00
	100	4.42	19.89	0.50	1.50
	200	8.630	42.38	1.85	2.55
	300	21.06	111.47	3.83	4.38
	400	46.05	273.47	4.64	5.44
	500	58.69	459.27	6.10	7.10
1.0	0	0.00	0.00	0.00	0.00
	100	0.82	4.13	0.78	1.29
	200	6.02	30.32	2.85	3.17
	300	14.35	71.64	3.79	4.05
	400	26.66	134.21	4.83	5.21
	500	31.40	150.68	5.89	6.28

Table 4.4 The comparison of deflection angle (θ) and the dielectrophoresis force (F_d) of the 3% wt BPO cPCL and other electroactive materials

Samples	**Electrical yield strength (V/mm)**	**θ (°)**	**F_d (mN)**	**Reference**
3% wt BPO cPCL	100	58.7	0.459	
1.0% v/v PPP/cPCL	100	31.5	0.222	
SAR	250	33.4	0.275	Kunanuraksapong *et al.*, 2007
SIS	400	11.0	0.071	
SBR	375	8.6	0.157	

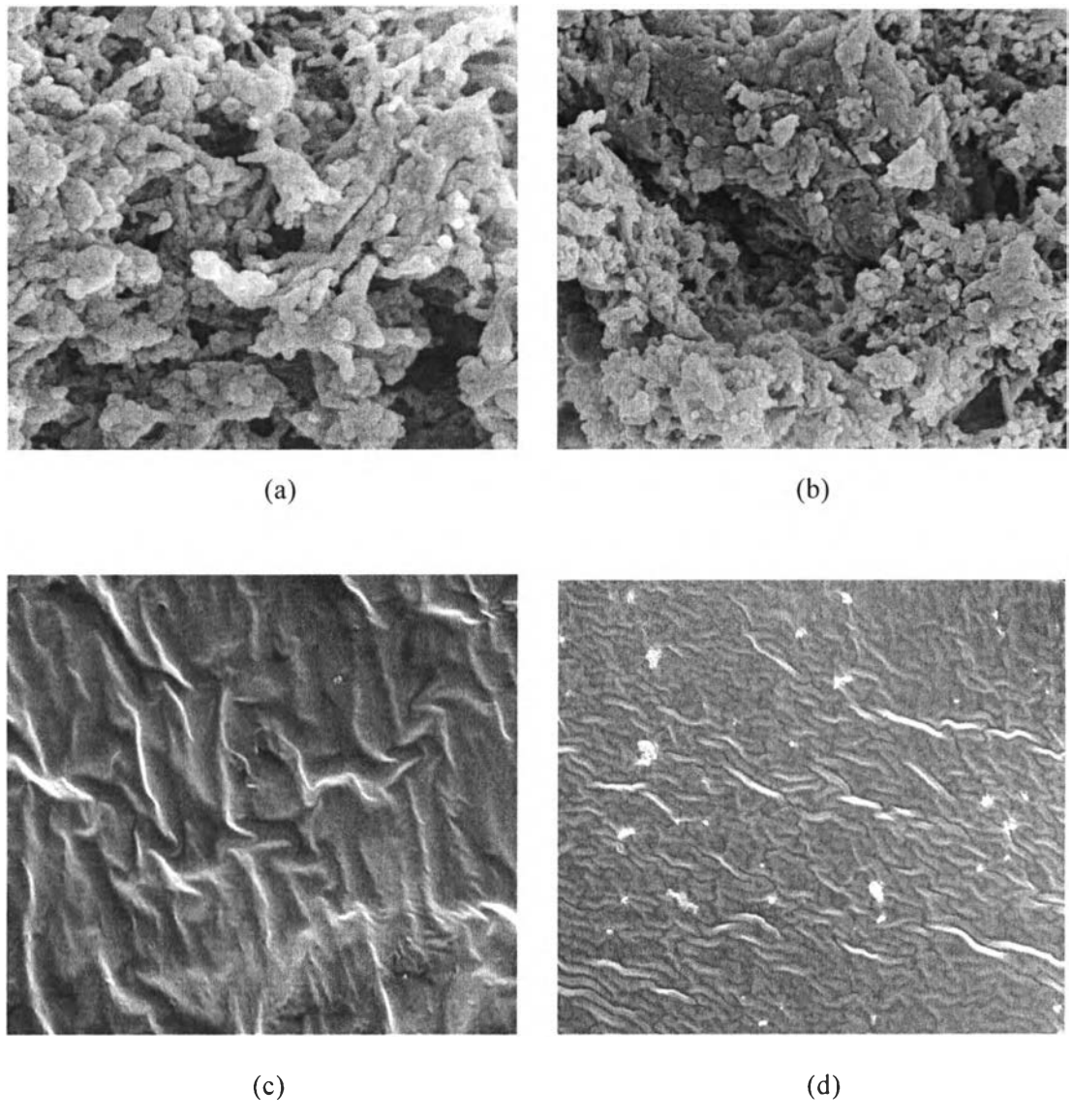

Figure 4.1 The morphology of: a) undoped; b) $FeCl_3$ doped PPP particle in the mole ratio between $FeCl_3$ and PPP monomer of 30:1 at the magnification of 20 kX; c) 3%wt BPO cPCL; d) 1.0% v/v 30:1 dPPP/3%wt BPO cPCL composite at the magnification of 1.5 kX.

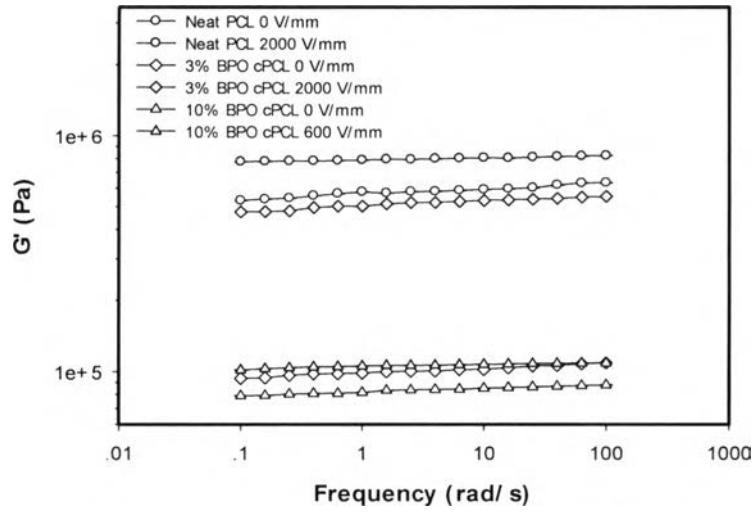

Figure 4.2 Storage modulus versus frequency of uncrosslinked PCL and crosslinked PCL at the various crosslinking ratios with and without 2 kV/mm of electric field, % strain 0.03, 25°C.

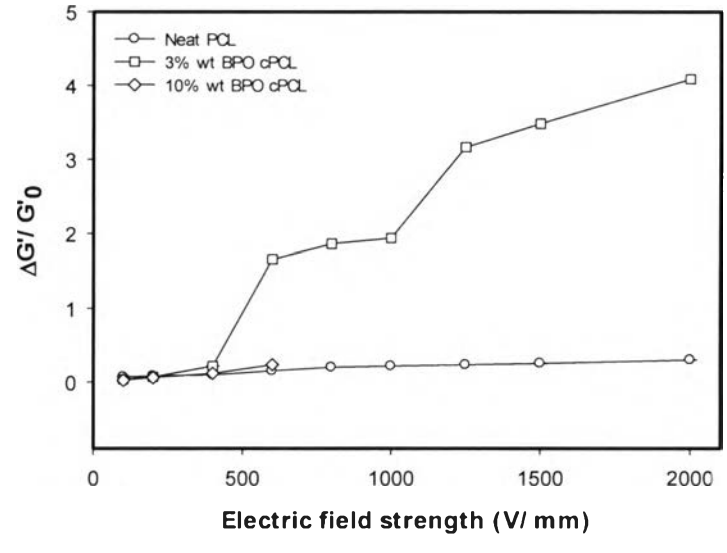

Figure 4.3 The comparison of the storage modulus sensitivity ($\Delta G'/G'_0$) as a function of electric field strength from 0 to 2 kV/mm of PCL films at the various crosslinking ratios, % strain 0.03, 25°C.

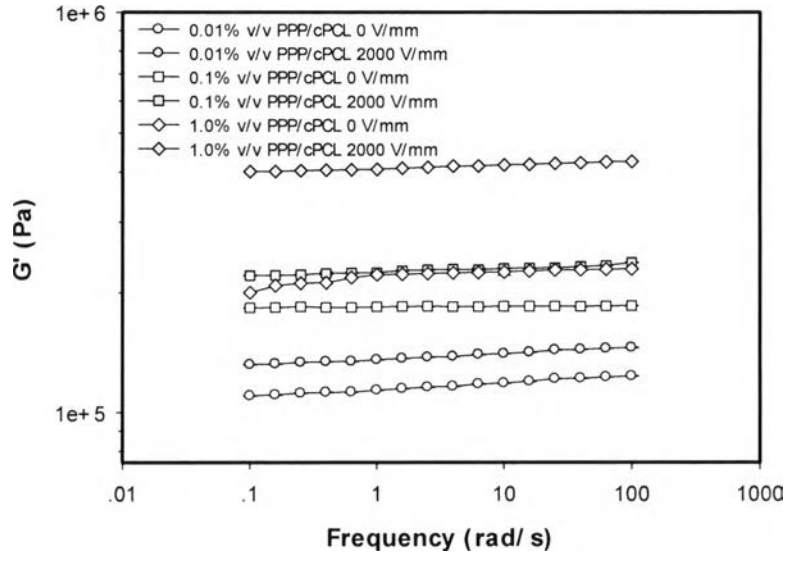

Figure 4.4 Storage modulus versus frequency of PPP/PCL composites at various PPP compositions with and without 2 kV/mm of electric field, % strain 0.03, 25°C.

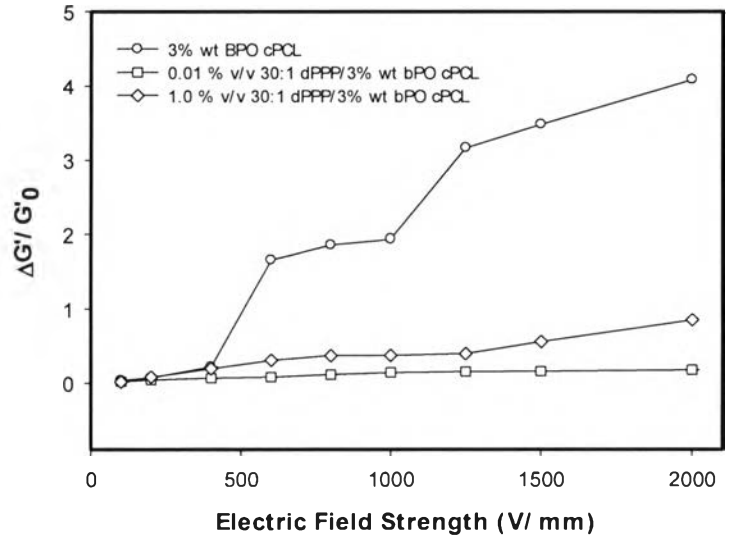

Figure 4.5 The comparison of storage modulus sensitivity ($\Delta G'/G'_0$) as a function of electric field strength from 0 to 2 kV/mm of PPP/PCL composites at various PPP compositions, % strain 0.03, 25°C.

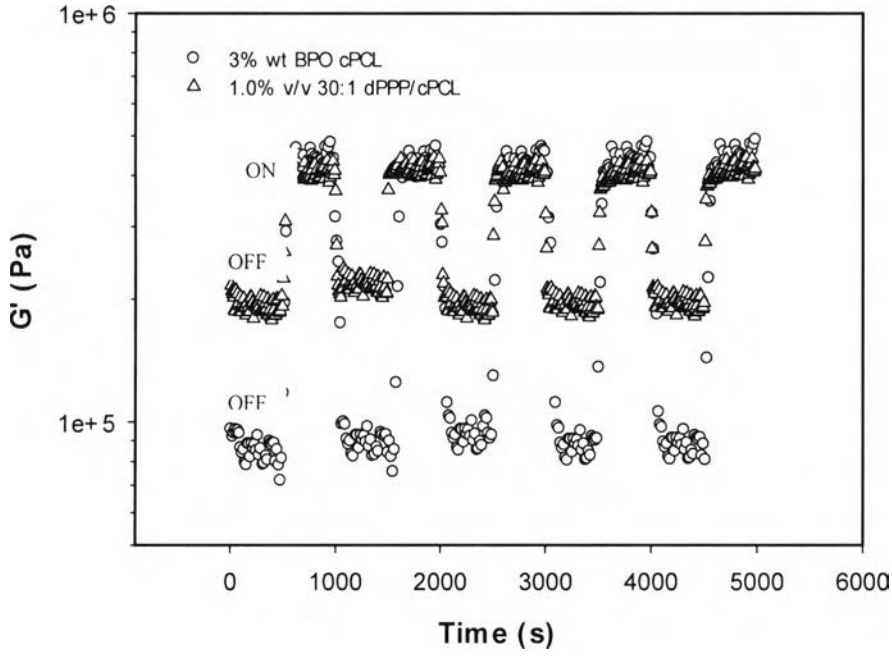

Figure 4.6 Temporal response of 3%wt BPO cPCL and 1.0% v/v 30:1 dPPP/ 3 % wt BPO cPCL, frequency 1 rad/s, %strain 0.03, 25°C.

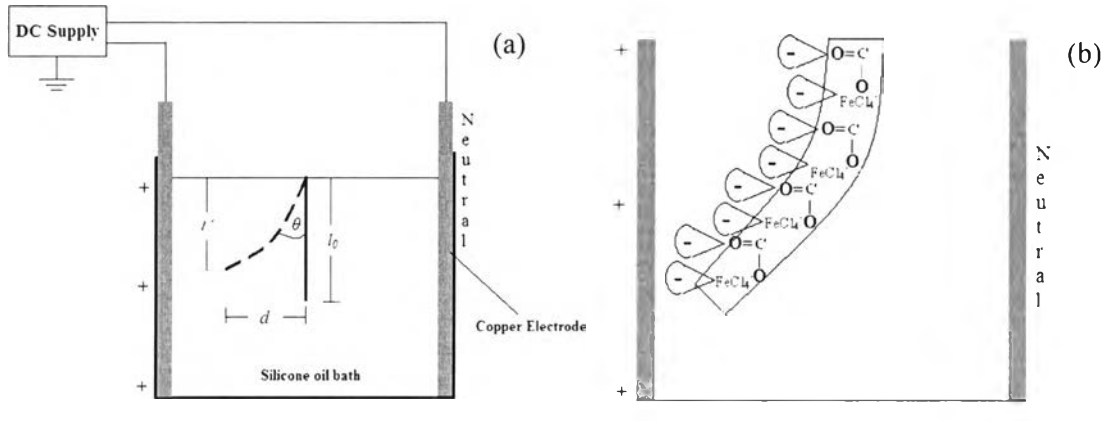

Figure 4.7 A schematic diagram of: a) The apparatus for deflection experiment which was deployed to observe the dielectrophoretic behavior of PCL films and PPP/PCL composites. The samples were immersed vertically in a silicone oil bath in which a DC electric field was applied through parallel copper electrodes; b) The actuation mechanism of PCL film and PPP/PCL.

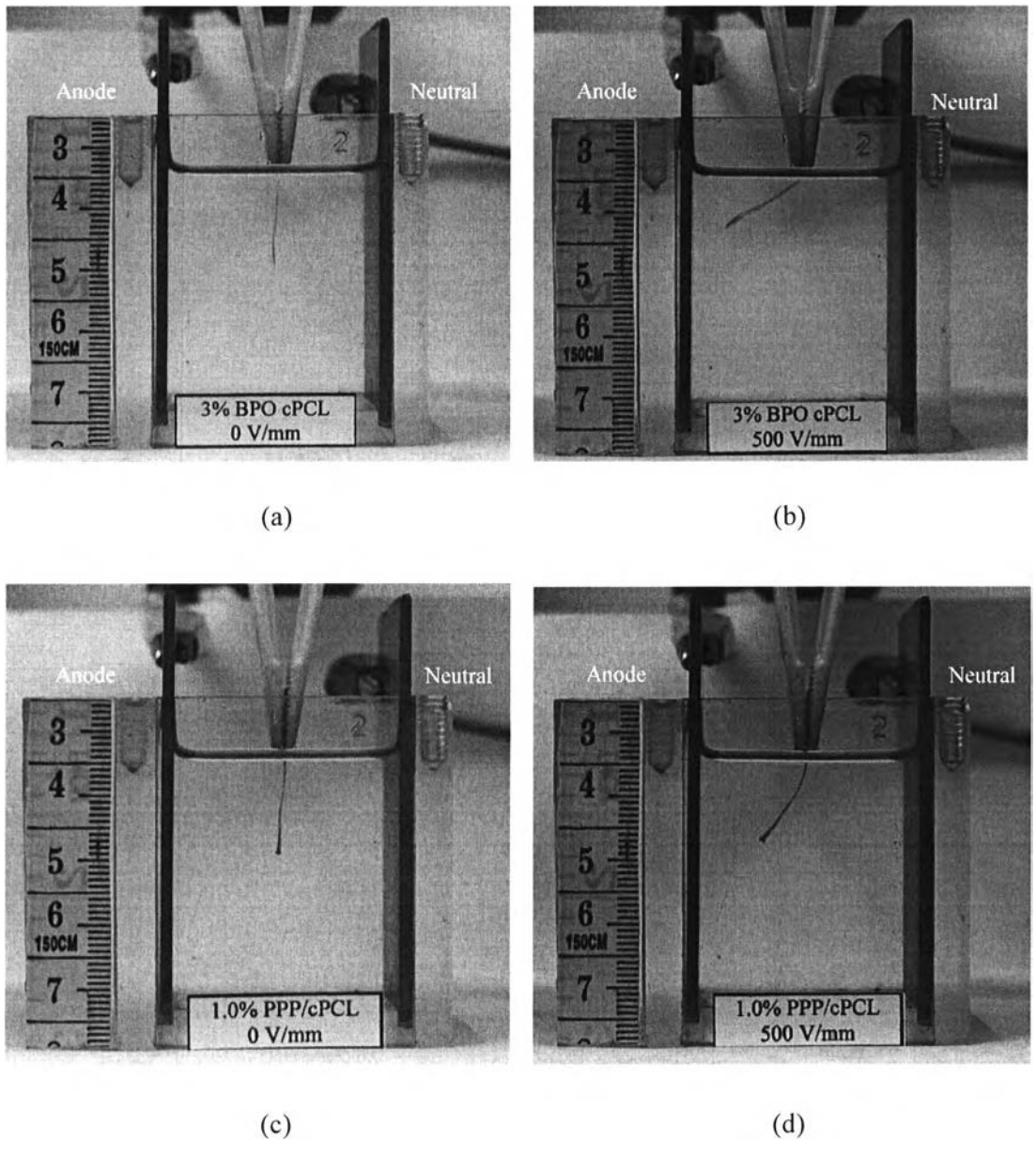

Figure 4.8 Photographs of the bending experiment of 3% wt BPO cPCL at the electric field strength ofs: a) 0 V/mm; b) 500 V/mm and 1.0% v/v 30:1 dPPP/3%wt BPO cPCL at the electric field strengths of: c) 0 V/mm; d) 500 V/mm.